RESILIENT INFRASTRUCTURE
June 1–4, 2016

EFFECT OF SUPPLEMENTARY CEMENTITIOUS MATERIALS ON THE RESISTANCE OF MORTAR TO PHYSICAL SULFATE SALT ATTACK

Semion Zhutovsky
University of Toronto, Canada

R. Douglas Hooton
University of Toronto, Canada

ABSTRACT

Physical sulfate salt attack is one of the most rapid and severe deterioration mechanisms in concrete structures. One of the most common approaches to improve resistance of concrete to sulfate attack is to use supplementary cementitious materials. However, physical salt attack may still cause damage to concrete with supplementary cementitious materials. Moreover, according to some literature sources, some supplementary cementitious materials may even reduce resistance to physical salt attack. The current research investigates the effect of supplementary cementitious materials on the ability of mortars to resist physical sulfate salt attack and its relationship with pore structure and transport properties. Mortar specimens with 45 and 65% replacement of cement by ground-granulated blast-furnace slag and with 20 and 40% replacement of cement by fly ash were exposed to physical sulfate attack. The results show a good correlation between the pore microstructure and transport properties to the resistance to physical salt attack. Ground-granulated blast-furnace slag was found to improve the resistance to physical salt attack, while fly ash demonstrated a negative effect.

Keywords: Sulfate attack; Physical salt attack; Durability; Supplementary Cementitious Materials;

1. INTRODUCTION

Sulfate attack may cause severe damage to concrete structures. Sulfate attack can take several forms (Hooton, 2015). Physical sulfate salt attack (PSA) and chemical sulfate attack are often confused (Haynes, et al., 1996). PSA involves crystallization and phase transitions of sulfate salts in the pores of a cementitious material as opposed to chemical sulfate attack, which is caused by chemical interaction between sulfate salts and cement minerals (Haynes, et al., 1996). The terms “salt scaling” and “salt weathering” are often used to designate PSA (Mehta, et al., 2006). Major efforts have been directed toward researching sulfate attack in concrete since 1920. However, the mechanisms of PSA were largely overlooked (Haynes, et al., 2008). The Portland Cement Association states that PSA causes damage, which is more severe than the damage caused by chemical sulfate attack (Stark, 2002). Another possible explanation is that increased early-age carbonation of inadequately cured SCM concretes maybe the reason of reduced resistance to PSA (Yoshida, et al., 2010), (Liu, et al., 2014).

At the present time, there is no standard method for evaluation of resistance of concrete to physical salt attack (Hooton, 2015). Concrete standards such as CSA A23.1 and ACI 318 simply (a) limit the maximum w/cm as an indirect way of limiting permeability, and (b) make use of test methods for evaluating the chemical resistance of the cementitious materials in the concrete. These current standard test methods (ASTM C452-15, 2015; ASTM C1012-15, 2015) are oriented to the testing of the resistance of cementitious materials to chemical sulfate attack, using the expansion of mortar bars as a measure of deterioration. However, PSA is often not accompanied by expansion. The PSA damage typically takes the form of surface scaling, which is similar to the damage caused by freezing and thawing (Haynes, et al., 1996). This is because PSA causes damage by means of the cycles of crystallization, dissolution and phase transitions of sulfate salts (Folliard, et al., 1994). To activate these mechanisms either drying or thermal cycles are needed.

Different exposure conditions, involving various combinations of drying and thermal cycles for the testing of PSA resistance of concrete, are reported in the literature (Haynes, et al., 2011). Thermal cycling between 5 and 30 °C in 30% sodium sulfate solution is reported as the one of the most severe exposures due to rapid crystallization of mirabilite (Folliard, et al., 1994). Mass loss from such exposure is rapid and may lead to complete disintegration. For this reason, this exposure condition was selected for the current study.

The objective of the current research is to evaluate the effect of SCM on the ability of mortars to resist physical salt attack, as well as to study the mechanisms of physical salt attack and the relationship with pore structure and transport properties imparted by the cementitious materials with SCM. For this purpose, mortars with w/cm ratio of 0.40 were tested, which complies with requirements of the current Canadian standard for most severe conditions of exposure to sulfate salts (CSA A23.1-14, 2014). The replacement levels of cement by FA of 20 and 40% were tested, GGBFS, subjected to the selected exposure conditions. Mortars were preferred over concrete because of higher permeability, which shortens the testing time, and over cement paste because of the presence of interfacial transition zones. High-sulfate resistant portland cement was used in all mixtures to reduce the possibility of chemical interaction between cement and sodium sulfate.

The results show a good correlation between the pore threshold radius using MIP and the resistance to physical salt attack, as well as between the chloride migration coefficient and the rate of deterioration in physical salt attack. Ground-granulated blast-furnace slag was found to improve the resistance to physical salt attack, while fly ash demonstrated a negative effect.

2. MATERIALS AND METHODS

2.1 Materials

Natural glacial sand of mixed mineralogy from Sunderland Pit, Ontario, Ontario Canada was used in all mortars at a constant 45% by volume. High sulfate-resistant cement from Lafarge was used in all mixes in order to reduce the possibility of chemical sulfate attack. SCMs used in this research were Holcim GGBFS, from Ontario, and FA type F from Avon Lake, Ohio, USA.

The effects of w/cm ratio, and cement replacement by SCM, GGBFS and FA, on the resistance of cement mortar to PSA were investigated. The effect of SCM on PSA was studied on mortars with w/cm ratio of 0.40. The replacement levels of cement by SCM studied were: 45 and 65% for GGBFS, and 20 and 40% for FA. The mix designs for tested mortars are shown in Table 1.

Table 1. Mix proportions [kg/m^3]

Mix Notation	W/CM	SCM Content, %		Cement	Water	Slag	FA	Sand
		Slag	FA					
M40	0.40	0	0	755	302	0	0	1182
SG45	0.40	45	0	406	295	332	0	1182
SG65	0.40	65	0	256	292	475	0	1182
FA20	0.40	0	20	594	297	0	148	1182
FA40	0.40	0	40	438	292	0	292	1182

2.2 Methods

Mortar prisms of 51×51×266 mm were used for studying the resistance to PSA, and 51 mm cubes were used for compressive strength and splitting tensile strength. All specimens were demolded at the age of 1 day and kept in saturated lime solution until 3 days. After 3 days of age the specimens were removed from the solution and kept in sealed conditions until the start of sulfate exposure at 28 days. According to (CSA A23.1-14, 2014) wet curing of 7 days is required only for extremely severe chloride exposure. For sulfate exposures (CSA A23.1-14, 2014) requires “additional” curing for the highest level of sulfates that corresponds to 7 days of curing, though no wet curing is required. Sealed curing would meet the CSA definition of additional curing. Thus the above curing conditions exceed

the “additional” curing requirements of (CSA A23.1-14, 2014) providing wet curing until the age of 3 days and sealed curing until the age of 28days, but would likely be inferior to “extended” curing.

Sulfate exposure involved thermal cycles of mortar prisms submerged in sodium sulfate solution. Thermal cycles were between 4 ±1 and 32 ±2 °C with maximum cooling and heating rates of 2.5 and 4 °C/h, respectively. The duration of one full thermal cycle was 24 hours. The concentration of sodium sulfate solution was 30% by mass and the solution was replaced every 5 cycles. The damage caused by PSA was assessed by means of mass loss on three replicate specimens. The measurements were taken every 10 cycles.

To study the pore structure at the age of 28 days, 51 mm cube specimens were crushed and sieved to a particle size between 2 and 2.5 mm and then submerged in propanol-2 solvent in order to stop hydration. The solvent was changed 3 times every hour and then specimens were kept immersed in the solvent for an additional 24 hours. After that, specimens were vacuum dried to constant mass for at least 24 hours. Pore structure was examined by means of mercury intrusion porosimetry (MIP). MIP tests were performed using a porosimeter with a maximum pressure of 415 MPa (60,000 psi). . The contact angle was taken as 140 ° in all pore size calculations. Threshold pore diameter, critical pore diameter and total porosity were extracted from the MIP data.

Non-steady-state chloride migration tests were performed at the age of 28 days according to a Scandinavian standard (NT BUILD 492, 1999). Chloride migration coefficients were measured on three 50 mm specimens cut from the top, middle and bottom part of three different cylinders of 200 mm height and 100 mm diameter.

The compressive strength and splitting tensile strength were measured at the ages of 1, 3, 7, 28 and 91 days. Three and five duplicate specimens were used at every age for testing compressive and splitting tensile strength, respectively. The standard deviation was in the range of 4-10% and 3-7% for splitting and compressive strengths, respectively.

3. EXPERIMENTAL RESULTS

3.1 Mass loss

The mass losses of the mortar prisms due to PSA are given in Figure 1. It can be seen that the mass loss didn’t start immediately. Initially a small weight gain was observed in most mixtures due to absorption of sulfate solution. After an initial period of 10-20 thermal cycles, the mass loss started and deterioration of the samples began in the form of scaling. The final mass loss, after 100 thermal cycles in 30% sulfate solution ranged between 10.7 and 41.5 % for the tested mixes.

In the beginning of sulfate exposure, mass loss in the mixes with slag was slightly higher than in the sulfate resistant cement reference mix. However, the rate of mass loss of the reference mix exceeded the mass loss of the mixes with slag at later stages. The mortar with 65% cement replacement by slag behaved slightly better that the mortar with 45% slag, but the difference in performance between the mixes was small.

Mortar mixes with fly ash exhibited considerably higher mass loss than the reference mix. However, the slope of mass loss decreased at later stages of thermal cycling. The difference between mixes with 20 and 40% of FA also changed during the course of testing. Initially the mortar with 40% FA demonstrated slightly higher mass loss than the mortar with 20% FA, though the final mass loss after 100 thermal cycles was the opposite.

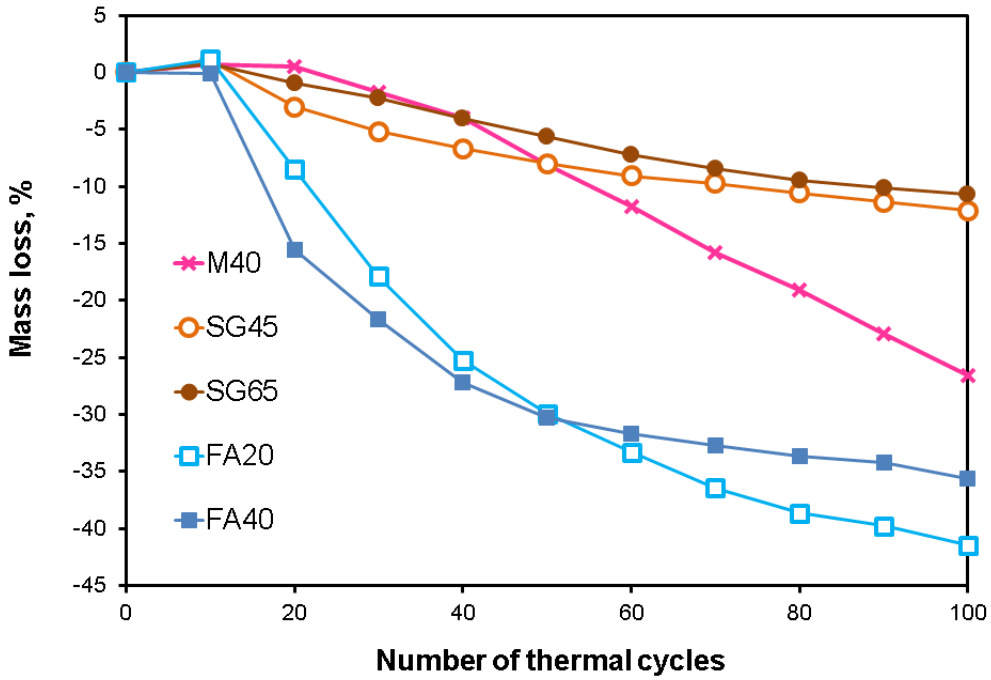

Figure 1: Mass loss

3.2 Pore structure

The total porosity, critical pore diameter and threshold pore diameter of mortars at 28 days, obtained by means of MIP, is presented in Figure 2 and Figure 3 for mortar mixes with GGBFS and FA, respectively. Total porosity was determined as the total intruded volume of mercury per sample volume. The threshold pore diameter is determined as the first inflection point in the MIP intrusion curve, and the critical pore diameter as the point of steepest slope. The threshold pore diameter denotes the beginning of the percolation of pore structure. On the other hand, the critical pore diameter allows maximum percolation throughout the pore system, which corresponds to the mean size of pore entryways (Mindess, et al., 2003).

The total porosity ranged from 10.5% in the M40 mortar mix to 14.7% in the SG65 mortar mix. The threshold pore diameter ranged from 0.028 μm in the SG45 mortar mix to 0.078 μm in the FA40 mortar at 28 days. The critical pore diameter ranged from 0.013 μm in the SG65 mortar mix to 0.024 μm in the FA40 mortar at 28 days.

The replacement of cement by slag resulted in increased total porosity: the higher the replacement level the higher the total porosity. However, the threshold diameter was significantly lower in the GGBFS mortars, although the threshold pore diameter of the mix with 65% slag was higher than in the mix with 45% slag. Critical pore diameter consistently decreased with the content of slag. This means that mortars with slag have higher but finer connected porosities compared to the reference cement mix.

The use of FA as cement replacement resulted in increases to total porosity and to both critical and threshold pore diameters: the higher the FA content the higher the increase in total porosity, critical, and threshold pore diameters. Thus, use of this FA resulted in higher porosity and a coarser, connected pore structure.

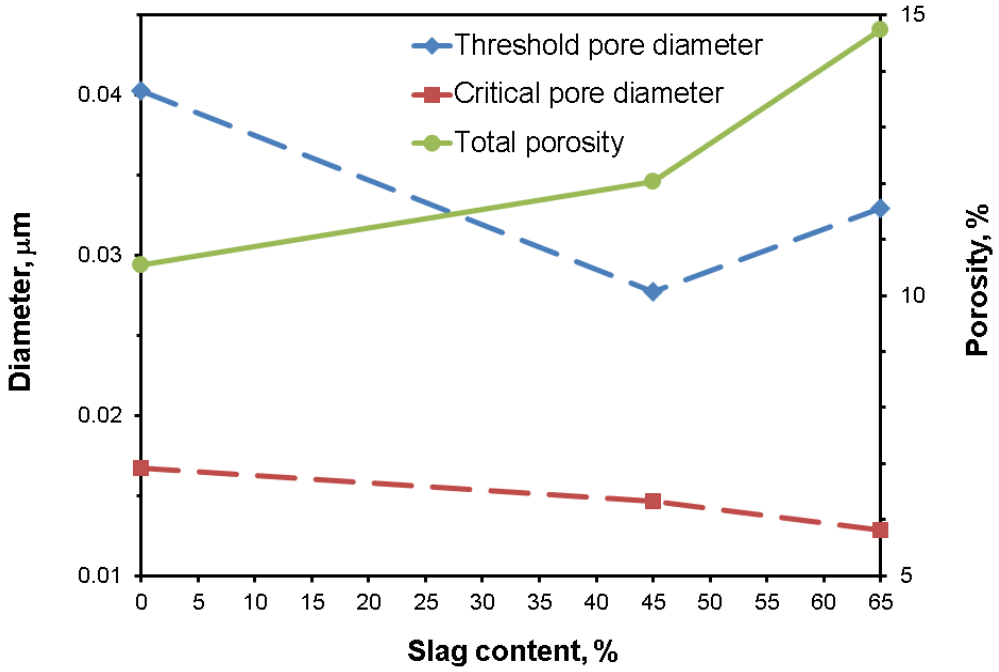

Figure 2: Pore structure parameters of mortar mixes with GGBFS

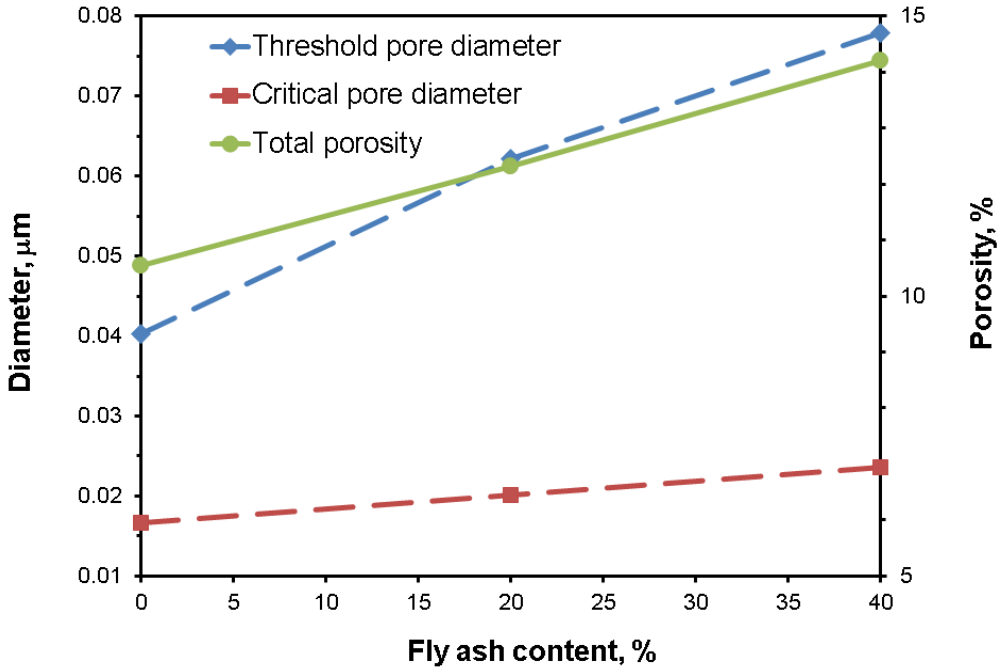

Figure 3: Pore structure parameters of mortar mixes with

3.3 Transport properties

In order to characterize the transport properties of the mortars, non-steady state chloride migration coefficients were measured using the NT Build 492 standard (NT BUILD 492, 1999). This test was used since there is no standard test for measuring sulfate ingress, and increased resistance to chloride penetration is likely similar to that of sulfate penetration if one neglects differences in binding. The effect of supplementary cementitious materials on chloride

migration coefficient is shown in Figure 4. The chloride migration coefficients ranged from 22.5×10^{-12} m^2/s in the FA40 mortar to 2.6×10^{-12} m^2/s in the SG65 mortar.

It can be seen in Figure 4 that the use of slag resulted in a drastic reduction in transport properties of the mortars. The chloride migration coefficient decreased steadily with the increase of slag content.
On the contrary, the introduction of FA into the mortar mix resulted in increased transport properties. Chloride migration coefficient increased in the mortars with FA nearly proportional to the content of FA.

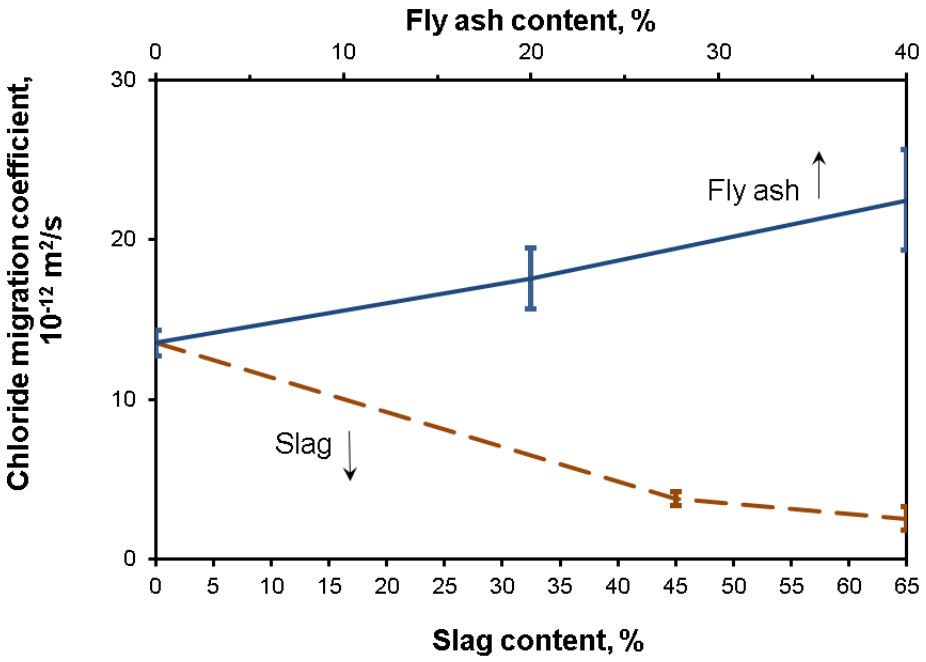

Figure 4: Effect of supplementary cementitious materials on chloride migration coefficient

3.4 Strength

Compressive and splitting tensile strengths are shown in Figure 5 and Figure 6, respectively. It can be seen that the replacement of cement by SCM reduces both compressive and splitting tensile strength at early ages: the higher the replacement level, the higher the reduction of strength. The development of compressive strength in mortars with SCM lagged behind the reference mortar even at later ages. Only the mortar mix with 45% slag slightly exceeded the compressive strength of the reference mix at 91-days. The tendency in splitting tensile strength is similar, with only the mortar mixes having 45% slag and 20% FA exceeding the splitting tensile strength of the reference mix at 91 days. However, the difference in the splitting tensile strength at later ages between the mixes is less significant than with compressive strength.

At early ages (1-3 days), the mortar mixes with GGBFS demonstrated lower compressive strength than the mixtures with FA. However, at later ages (28-91 days) the mixes with slag demonstrated better performance than mixes with FA. It is known that the mixes with SCM require longer curing than the mixes with unblended Portland cement. Thus it is possible that prolonged curing will improve the strength development in the mixes with SCM. When used in concrete, adjustments to mix proportions can be made to provide equal strength at early ages, but this was not done here.

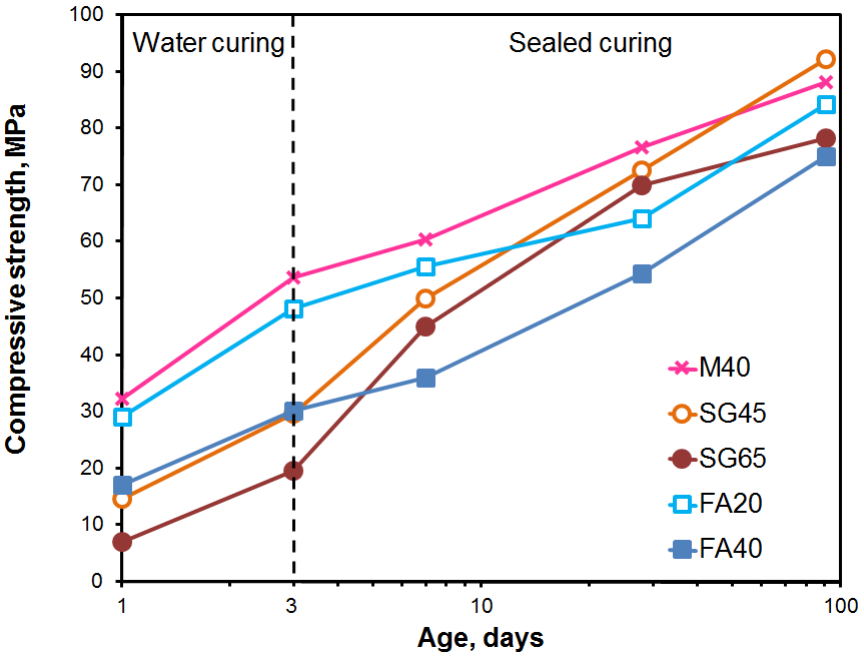

Figure 5: Effect of supplementary cementitious materials on compressive strength

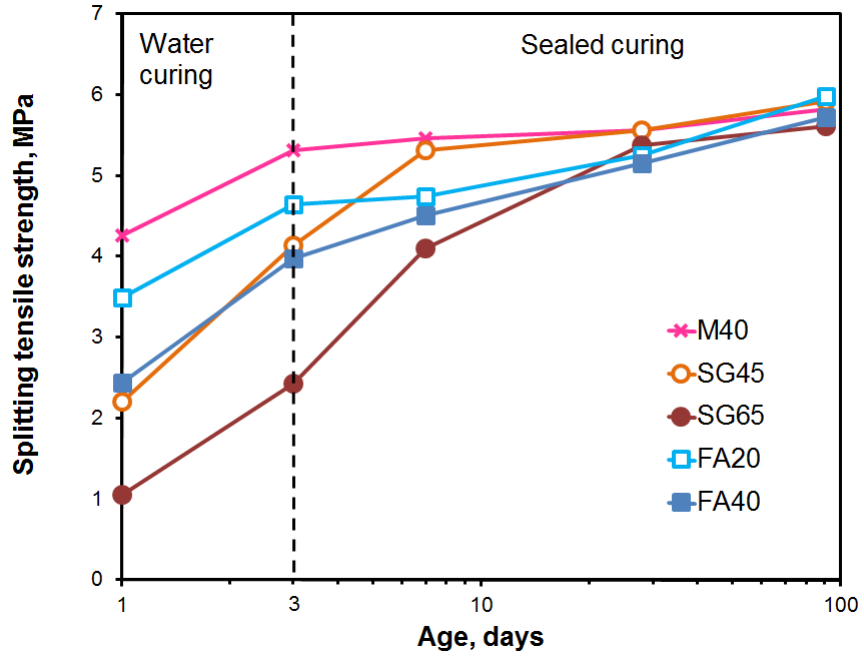

Figure 6: Effect of supplementary cementitious materials on splitting tensile strength

4. DISCUSSION

The effects of SCM on the mass loss due to PSA were shown in Figure 1. Though the general trend of the resistance of the mortars to PSA is clear from Figure 1, it is interesting to analyze the dynamics of the deterioration. The change in the rate of mass loss with the number of thermal cycles in sodium sulfate solution is shown in Figure 7. It can be seen that the initial short period of mass gain is followed by a steady increase in the rate of mass loss of all mixes. After the initial period of 20-40 cycles, the mortar mixes with SCM demonstrated decreased rates of mass loss.

The decrease in the rate of mass loss of the mortars with FA is the most significant, and most probably was caused by additional hydration of FA by virtue of additional water readily available from the sodium sulfate solution. Thus, the mixes with fly ash potentially can benefit from extended water curing. However, the replacement of cement by fly ash without sufficient water curing appears to increase PSA significantly. The initial rates of mass loss of the mortar mixes with GGBFS were lower, as compared to the mixes with FA. However, a reduction in the rate of mass loss at later stages was also observed in the mortars with slag. The mortar mixes with slag demonstrated the lowest deterioration in PSA. It can be concluded the use of slag is beneficial for resisting PSA.

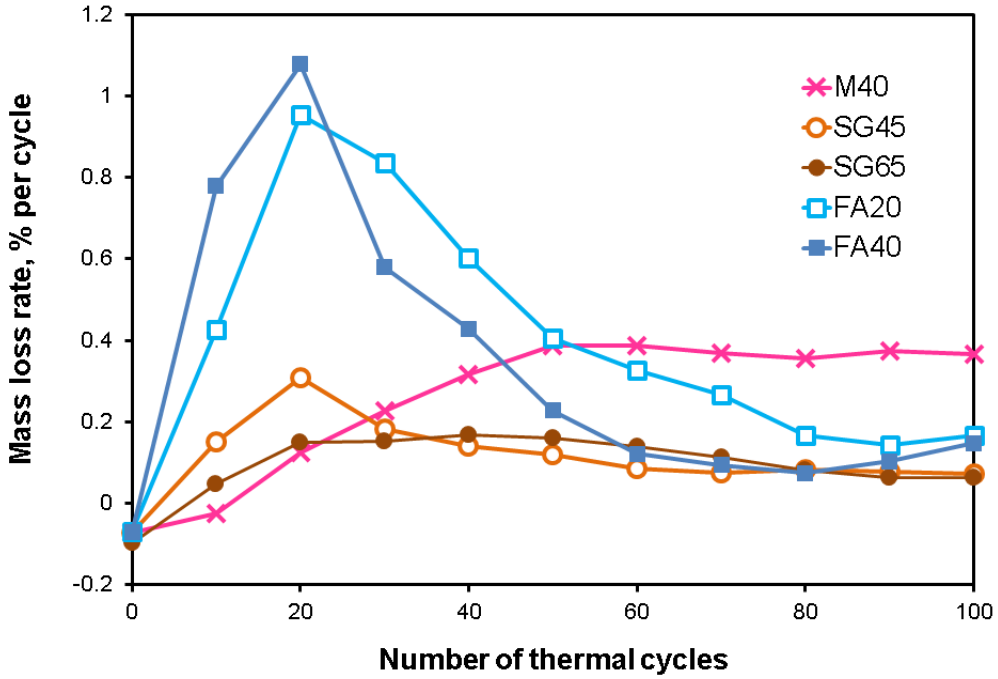

Figure 7: Effect of supplementary cementitious materials on rate of mass loss

The effect of SCM on the pore structure can be clearly seen in Figure 2 and Figure 3 for the mixes with GGBFS and FA, respectively. The question about the usefulness of MIP for pore structure analysis is the subject of much discussion. However, it is commonly agreed that some characteristic values of MIP curve such as the threshold or critical pore size can be related to transport properties such as permeability and diffusivity [16]. Indeed, as can be seen in Figure 8, a good correlation was obtained between the chloride migration coefficient and both the threshold and critical pore diameter.

If the mass loss of the mortar mixes after 100 cycles is plotted against the migration coefficient (see Figure 8), it can be seen that there is nearly linear trend between the final mass loss and the migration coefficient. The mortars with FA show some deviation from this trend. However, the continuous hydration of FA mixes during the period of the test needs to be considered as it probably caused refinement of pore structure and reduction of permeability, beyond those measured at the start of PSA exposure.

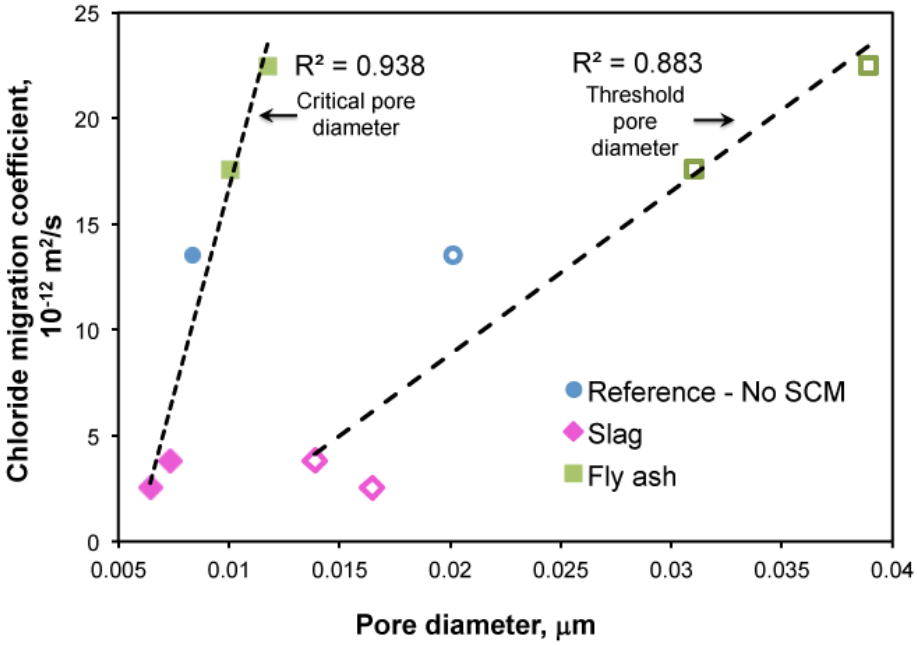

Figure 8: Correlation of transport properties and pore structure parameters

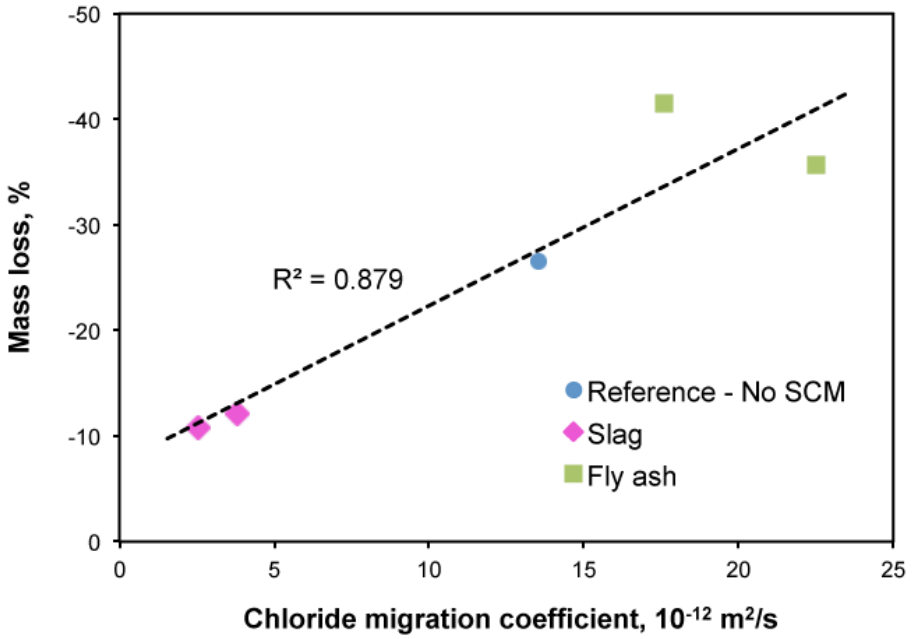

Figure 9: Correlation of transport properties and mass loss in PSA

It can be inferred that the rate of transport of sulfate ions through the pore system of cement paste is the main mechanism involved in degradation of cementitious materials due to PSA. This is why limits on maximum w/cm are required for concrete in sulfate exposure. The refinement of capillary pore structure and the resultant reduction in transport properties is the main way to control the resistance of concrete to PSA. It was found that an improvement of PSA resistance can be achieved by using GGBFS, which produced finer pore microstructure. However, FA, which produced a coarser pore microstructure, has demonstrated a negative effect on the resistance to PSA. However, further research is needed to investigate whether prolonged curing (beyond 3 days) is capable of improving the behavior of FA mixes to PSA. The results of strength tests, which were low as compared to the reference cement mix, also suggest that additional curing is needed.

It should be noted that the above findings are in contradiction with some of the previous studies about PSA resistance of SCM concrete mixes. Obviously the refinement of pore structure was not the reason of poor performance of SCM mixes. The possible reason for the difference in the SCM performance results is due to the effects of carbonation in some other studies. Due to the nature of curing and type of exposure in these experiments, carbonation was not a factor.

5. CONCLUSIONS

Summarizing the results, it can be concluded that:

1. The rate of PSA deterioration depends on the pore microstructure and transport properties of cementitious materials. Thus, the resistance to transport of sulfates is the primary mechanism controlling PSA damage.
2. The replacement of cement by GGBFS up to the level of 65% significantly improved the resistance to PSA. The improvement of the mortar resistance to PSA was achieved by refinement of the pore microstructure, although the total porosity in the mixes with GGBFS was higher.
3. The fly ash used had a detrimental effect on the resistance of mortars to PSA, though it is possible that performance of fly ash mixes can be improved by longer water curing. Further research is needed to confirm that insufficient curing is responsible for the poor behavior of fly ash mixes exposed to PSA.

REFERENCES

ACI 318-14, 2014. *Building Code Requirements for Structural Concrete and Commentary,* s.l.: American Concrete Institute.

ASTM C1012-15, 2015. *Standard Test Method for Length Change of Hydraulic-Cement Mortars Exposed to a Sulfate Solution,* s.l.: American Society for Testing and Materials.

ASTM C452-15, 2015. *Standard Test Method for Potential Expansion of Portland-Cement Mortars Exposed to Sulfate,* s.l.: American Society for Testing and Materials.

CSA A23.1-14, 2014. *Concrete materials and methods of concrete construction,* Toronto, Ontario, Canada: Canadian Standards Association.

Diamond, S., 2000. Mercury porosimetry. An inappropriate method for the measurement of pore size distributions in cement-based materials.. *Cement and Concrete Research,* 30(10), pp. 1517-1525.

Folliard, K. & Sandberg, P., 1994. *Mechanisms of concrete deterioration by sodium sulfate crystallization.* Nice, France, American Concrete Institute, pp. 933-945.

Haynes, H. & Bassuoni, M., 2011. Physical Salt Attack on Concrete. *Concrete International,* 33(11), pp. 38-42.

Haynes, H., O'Neill, R. & Mehta, P. K., 1996. Concrete Deterioration From Phusical Attack By Salts. *Concrete International,* 18(1), pp. 63-68.

Haynes, H., O'Neill, R., Neff, M. & Mehta, P. K., 2008. Salt weathering distress on concrete exposed to sodium sulfate environment. *ACI Materials Journal,* 105(1), pp. 35-43.

Hooton, R., 2015. Current developments and future needs in standards for cementitious materials. *Cement and Concrete Research,* Volume 78, pp. 165-177.

Irassar, E., Di Maio, A. & Batic, O., 1996. Sulfate attack on concrete with mineral admixtures. *Cement and Concrete Research,* 26(1), pp. 113-123.

Lea, F., 1998. *Chemistry of Cement and Concrete.* 3rd ed. New York: Chemical Publishing Co..

Liu, Z., Deng, D. & De Schutter, G., 2014. Does concrete suffer sulfate salt weathering?. *Construction and Building Materials,* 66(15), pp. 692-701.

Mehta, P. & Monteiro, P. J. M., 2006. *Concrete: Microstructure, Properties, and Materials.* 3rd ed. s.l.:McGraw-Hill.

Mindess, S., Young, J. & Darwin, D., 2003. *Concrete.* 2nd ed. Upper Saddle River, (NJ), USA: Prentice-Hall, Inc.,.

NT BUILD 492, 1999. *Concrete, mortar and cement-based repair materials: chloride migration coefficient from non-steady-state migration experiments.* s.l.:Nordic Counsil of Ministers.

Stark, D., 1989. *Durability of concrete in sulfate rich soils,* Skokie, Illinois, USA: Portland Cement Association.

Stark, D. C., 2002. *Performance of Concrete in Sulfate Environments,* Skokie, Illinois, USA: Portland Cement Association.

Verbeck, G. J., 1968. *Field and Laboratory Studies of the Sulfate Resistance of Concrete.* s.l., s.n.

Yoshida, N., Matsunami, Y., Nagayama, M. & Sakai, E., 2010. Salt weathering in residential concrete foundations exposed to sulfate-bearing ground. *Journal of Advanced Concrete Technology,* 8(2), pp. 121-134.